Available online at www.sciencedirect.com
ScienceDirect
Journal of Power Sources 176 (2008) 276–281
JOURNAL OF POWER SOURCES
www.elsevier.com/locate/jpowsour

Short communication

Carbon film-coated 304 stainless steel as PEMFC bipolar plate

Chih-Yeh Chung, Shi-Kun Chen *, Po-Jen Chiu, Ming-Hsin Chang, Tien-Tsai Hung, Tse-Hao Ko

Department of Materials Science and Engineering, Feng Chia University, Taichung 40724, Taiwan

Received 31 August 2007; received in revised form 8 October 2007; accepted 9 October 2007
Available online 13 October 2007

Abstract

Carbon film-coated stainless steel (CFCSS) has been evaluated as a low-cost and small-volume substitute for graphite bipolar plate in polymer electrolyte membrane fuel cell (PEMFC). In the present work, AISI 304 stainless steel (304SS) plate was coated with nickel layer to catalyze carbon deposits at 680°C under C_2H_2/H_2 mixed gas atmosphere. Surface morphologies of carbon deposits exhibited strong dependence on the concentration of carbonaceous gas and a continuous carbon film with compact structure was obtained at 680 °C under C_2H_2/H_2 mixed gas ratio of 0.45. Systematic analyses indicated that the carbon film was composed of a highly ordered graphite layer and a surface layer with disarranged graphite structure. Both corrosion endurance tests and PEMFC operations showed that the carbon film revealed excellent chemical stability similar to high-purity graphite plate, which successfully protected 304SS substrate against the corrosive environment in PEMFC. We therefore predict CFCSS plates may practically replace commercial graphite plates in the application of PEMFC.

Keywords: Polymer electrolyte membrane fuel cell; Carbon film; Bipolar plate; Corrosion resistance; Graphitization

1. Introduction

Polymer electrolyte membrane fuel cell (PEMFC) has attracted much attention in recent years as a result of its high efficiency in converting chemical energy into electric power at low temperature (70–90 °C) without polluted by-products [1]. The development of PEMFC is limited by some issues nowadays, notably the expensive cost [2] and the huge volume. A solution to these obstacles is to improve the properties of bipolar plate since it constitutes about 29% of the cost [3] and 95% of the volume in PEMFC. Graphite is employed to make bipolar plate in general due to its excellent natures in terms of chemical stability and electric conductivity, but its costs in material and machining gas channels are expensive and it needs a sufficient thickness for redeeming its poor mechanical strength so as to prevent crushing during PEMFC assembly process.

Carbon composite plate and alloy plate have been considered as alternatives to graphite plate [4–12]. The former shows significant advantages in cheap materials (carbon powers and polymer resin) and easy manufacture (hot press or injection molding), but its poor electric conductivity and mechanical strength handicap the scale-up of fuel cell stack [13]. As the most promising substitute, metallic plate shows properties essential to bipolar plate except chemical stability. Strong acidic environment in PEMFC stemming from perfluorosulfonic acid membrane dissociates metal ions, e.g. Fe, Cr and Ni ions, from metallic bipolar plate to contaminate polymer electrolyte and Pt catalyst. The declines in proton conductivity and catalyst activity eventuate in the collapse of PEMFC performance [14]. Special alloys as well as surface modification, therefore, have been investigated intensively for improving the anti-corrosivity of metallic bipolar plate [15,16].

A new approach is coating a carbon film on stainless steel substrate by thermal chemical vapor deposition (CVD), which may integrate the advantages of graphite into metallic bipolar plate. According to literature data [17], the major forms of carbon deposits are tubular or filamentous rather than a compact film. Hence, in this study a process to develop continuous carbon film on AISI 304 stainless steel (abbreviated as 304SS below) is investigated. We found that surface morphologies of the films are strongly dependent on the concentration of carbonaceous gas in the CVD process. The obtained samples were subjected

* Corresponding author. Tel.: +886 4 24512298; fax: +886 4 24510014.
E-mail address: skchen@fcu.edu.tw (S.-K. Chen).

0378-7753/$ – see front matter © 2007 Elsevier B.V. All rights reserved.
doi:10.1016/j.jpowsour.2007.10.022

to corrosion test and PEMFC performance analysis to compare with commercial graphite plate.

2. Experimental

2.1. Preparation and characterization of carbon film

As the catalyst in catalytic graphitization [18], 1 μm-thick nickel was applied to 304SS substrates by magnetron sputtering. Later on, these samples were placed in a tube furnace to develop carbon film at 680 °C under acetylene/hydrogen mixed gas atmospheres of three flow-rate ratios, 0.15, 0.45 and 1.5, which supplied carbon sources for the CVD process. Scanning electron microscope (SEM) was used to observe the morphology of the carbon deposits. In some cases, energy dispersion spectrometer (EDS) was performed with SEM. Glow discharge spectrometer (GDS) and dispersive Raman spectrometer were employed to determine the composition-depth profile and carbon structure of the carbon film.

2.2. Corrosion endurance tests

Corrosion tests were carried out at room temperature via potentiodynamic polarization techniques in an undivided three-electrode glass cell (250 cm^3 in volume) with a Pt mesh (110 cm^2) auxiliary electrode and an Ag/AgCl (saturated KCl) reference electrode. Samples (working electrodes) were mounted on this cell and subjected to 0.5 M H_2SO_4 solution to simulate the corrosive environment in PEMFC [19,20]. Potentiodynamic polarization curves were recorded with a CHI potentiostat (model 6081C) at a scan rate of 10 mV s^{-1} from −1.0 to 2.0 V (versus normal hydrogen electrode, or NHE). After the corrosion tests, the concentration of metal ions in each H_2SO_4 test solution was gauged with induced coupled plasma-mass spectrometer (ICP-MS).

2.3. Fuel cell tests

Carbon electrodes (A-6 ELAT®, E-TEK) with Pt loading of 0.4 mg cm^{-2} were employed as anodes and cathodes. A thin layer of Nafion (3 mg cm^{-2}) solution was spread on the electrode surface before making membrane electrode assemblies (MEA). MEAs with active area of 4 cm^2 were obtain by pressing anode and cathode on either side of Nafion 117 membrane (DuPont) under 55 kg cm^{-2} at 140 °C for 1 min. Each MEA was activated and tested for 8 h in a standard fuel cell tester to ensure the same performance. Specimens with identical gas flow channels were assembled with MEA to form fuel cell modules, which were connected to PEMFC performance testing system (e-load 6060B, Agilent) for the 100-h operation at 0.6 V and 40 °C with flowing humidity-saturated H_2 and O_2 in anode and cathode, respectively.

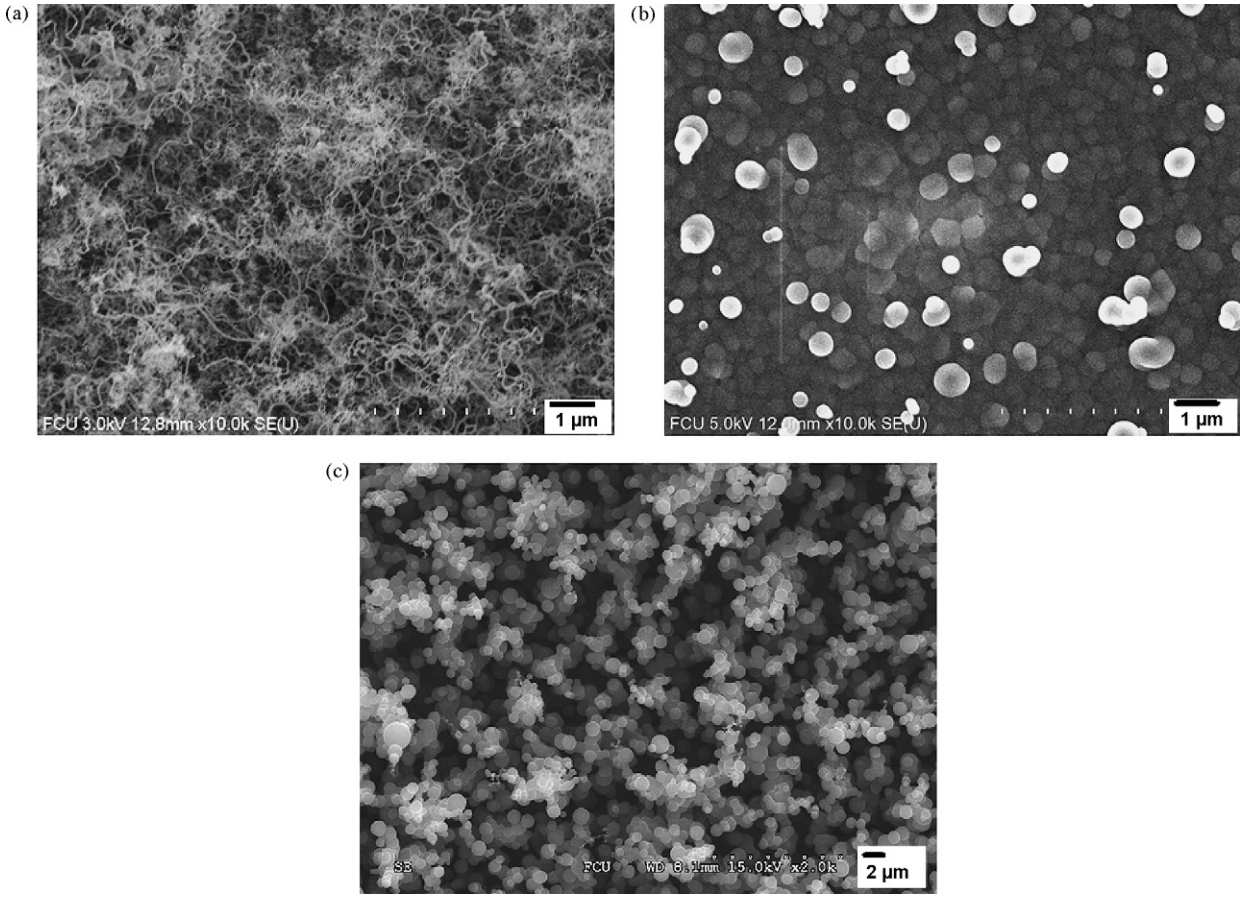

Fig. 1. SEM images of the surface morphology of the specimens prepared at 680 °C under C_2H_2/H_2 ratio of (a) 0.15, (b) 0.45 and (c) 1.5.

3. Results and discussion

3.1. Influence of the ratio of C_2H_2/H_2 mixed gas on the morphology of carbon deposits

In all the specimens investigated, surface morphologies of the carbon deposits are strongly dependent on the ratio of C_2H_2/H_2 mixed gas. As the SEM images depicted in Fig. 1, the surfaces of specimens prepared under C_2H_2/H_2 ratio of 0.15, 0.45 and 1.5 are individually covered with filamentous carbon, carbon balls and carbon-ball clusters.

Fig. 1(a) shows a morphology very similar to the result of Ref. [17], i.e. carbon molecules decomposed from C_2H_2 diffuse to specimen surface and are transformed to graphite by the catalysis of Ni layer [21,22]. Subsequently coming carbon molecules follow the graphite texture to arrange in order and make the graphite film thicker (epitaxial effect). According to a prior study by Chun et al. [23], however, highly ordered graphite film provides the interspaces between (0 0 2) graphite basal planes as channels for the migration of Ni atoms from Ni underlayer to the surface of graphite film, where Ni atoms coalesce to small particles and catalyze the subsequently coming carbon molecules to form filamentous carbon. A sketch describing the mechanism is shown in Fig. 2.

Fig. 1(b) and (c) indicates that carbon balls displace filamentous carbon as composed unit of the coatings while C_2H_2/H_2 ratio is increased to 0.45 or even 1.5. We thus assume that the increase in carbon source concentration is accompanied with the development of carbon balls. It seems that C_2H_2/H_2 mixed gas ratio of 0.45 provides an ideal carbon source in which carbon balls stack densely to form continuous and compact film on the substrate, showing mirror-like smoothness. By contrast, a loose coating composed of carbon balls is observed on the specimen prepared at C_2H_2/H_2 mixed gas ratio of 1.5. Owing to this uneven stacking of carbon balls, it is believed that carbon balls congregate to form clusters in advance of depositing on specimen surface. This phenomenon might arise from the extremely high-concentration carbon source bringing a large number of carbon balls which collide with each other at high probability in the boundary layer and form the stable structure of carbon-ball cluster due to the decrease in surface free energy.

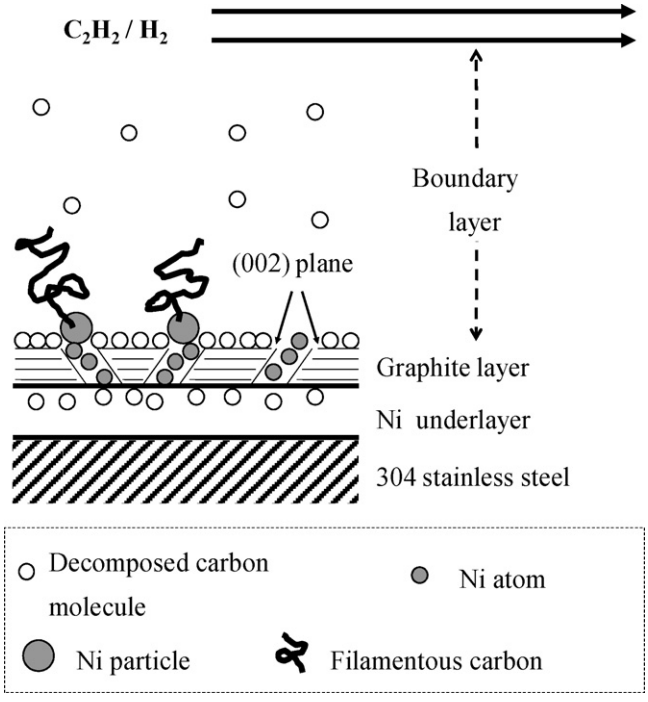

Fig. 2. Schematic representation of the development of filamentous carbon at 680 °C under C_2H_2/H_2 ratio of 0.15.

3.2. Characterizations of the carbon film

Since the specimen prepared under C_2H_2/H_2 mixed gas ratio of 0.45 exhibits significantly different surface morphology from filamentous carbon, it is interesting to investigate the carbon film in terms of structure and growth mechanism. SEM image of the carbon/Ni interface shown in Fig. 3 displays a tightly compact structure existing in the carbon film. It is worth to note that there are three bright regions larger than 250 nm inside the carbon film, identified as Ni precipitates by EDS analyses. These precipitates appear at similar distances from the carbon/Ni interface. The composition-depth profile shown in Fig. 4 demonstrates the concentration of Ni gradually decreasing from the carbon/Ni interface toward the specimen surface, but there is an abrupt rise at about the middle of the carbon film. This unusual phenomenon precisely corresponds to the appearance of Ni precipitates in the carbon film as described in Fig. 3.

On the basis of the above results, a probable growth mechanism to the carbon film is diagrammed in Fig. 5 and detailed as follows: at the outset of the CVD process, carbon balls are transformed to a highly ordered graphite layer at the carbon/Ni interface through the catalysis of Ni underlayer. This graphite layer provides some interspaces between (0 0 2) basal planes as channels for the migration of Ni atoms. This phenomenon is similar to the initial development stage of filamentous carbon. However, C_2H_2/H_2 mixed gas ratio of 0.45 provides an ideal

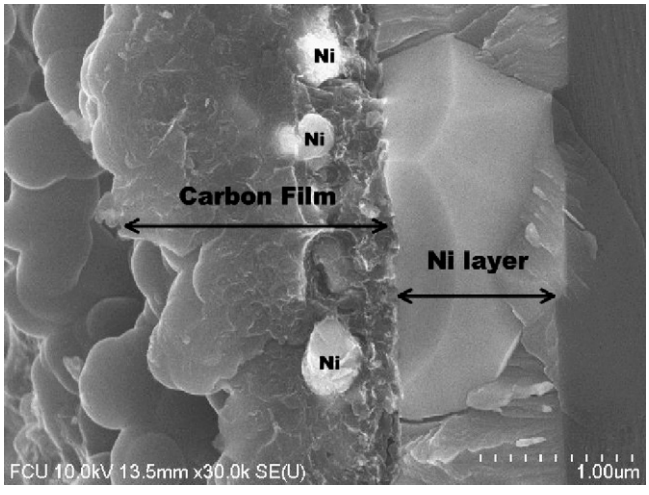

Fig. 3. Cross-section SEM image of the carbon film developed at 680 °C under C_2H_2/H_2 ratio of 0.45 showing the obvious carbon/Ni interface and three Ni precipitates inside the carbon film.

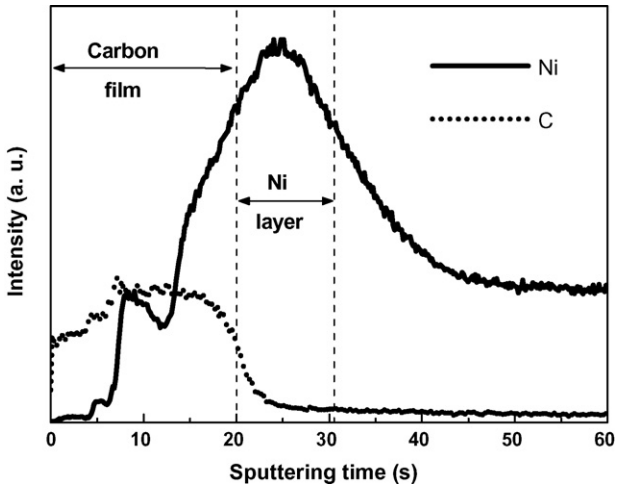

Fig. 4. Composition-depth profile of CFCSS plate showing the concentration of Ni abruptly rising in the carbon film. Solid and dotted lines represent the intensity of Ni and carbon, respectively.

carbon source in which the growth velocity of carbon film is higher than the migration velocity of Ni atoms. Ni atoms are thus unable to reach the surface of carbon film to catalyze filamentous carbon. As the carbon film thickens, the epitaxial effect of the graphite layer gradually becomes unapparent, resulting in more and more defects emerging in the surface layer of the carbon film. Defective graphite structures disorder the orientations of (0 0 2) basal planes, this makes Ni atoms ceaselessly coalesce at the ends of the migration paths to form huge precipitates.

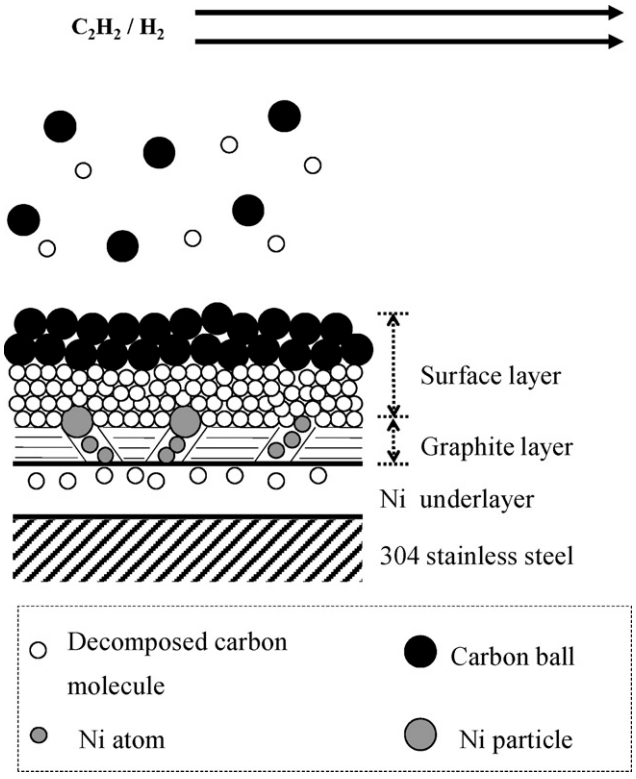

Fig. 5. Schematic representation of the development of carbon film at 680 °C under C_2H_2/H_2 ratio of 0.45 showing the coalescence of Ni atoms at the interface between the graphite and the surface layers.

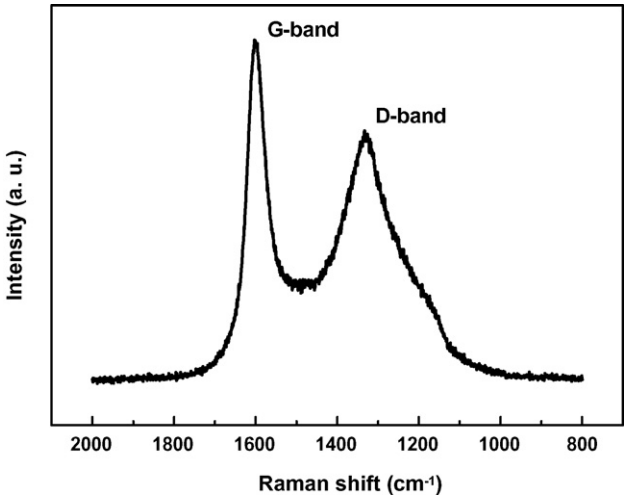

Fig. 6. Raman spectrum of the carbon film developed under C_2H_2/H_2 ratio of 0.45 at 680 °C.

Graphite structures in the carbon film are determined with Raman spectroscope, and the result shown in Fig. 6 corresponds to the above assumption. G-band and D-band individually represent the resonances of carbon atoms in ordered and defective graphite structure [24,25]. The strong intensity and the narrow full width at half maximum (FWHM) of G-band signify the carbon film containing an abundance of ordered graphite structures, which could be attributed to highly ordered graphite layer developed early in the CVD process. The broad FWHM of D-band denotes numerous disarranged graphite structures in the carbon film, which coincides with the above description to the development of the surface layer and further explains why Ni atoms cannot migrate through the surface layer.

3.3. Chemical stability analyses

Carbon film-coated 304SS (abbreviated as CFCSS below) plate is selected to compare with both commercial graphite plate (Poco AXF-5QCF) and 304SS plate in the corrosion endurance tests carried out via potentiodynamic polarization in 0.5 M H_2SO_4 solution since filamentous carbon or carbon-ball clusters are evidently unable to prevent the penetration of H_2SO_4 solution. Fig. 7 shows Tafel curves of CFCSS, 304SS and Poco graphite plates. CFCSS plate displays a redox peak at 1.6 V close to that of Poco graphite plate (1.4 V), so its chemical stability should be as passive as high-purity graphite in theory. The reaction potentials in PEMFC anode and cathode are individually at 0 and 1.229 V, both below the redox peak of CFCSS plate. Therefore, it can be asserted that corrosion reactions on CFCSS plate are very slight under PEMFC operating environment since CFCSS plate always retains in reduction state. By contrast, the reaction potentials in PEMFC are above the redox peak of 304SS plate appearing at −0.2 V, suggesting that the oxidation would predominate over the reduction on 304SS plate under PEMFC operating environment, i.e. the corrosion of 304SS bipolar plate is spontaneous.

After the corrosion endurance tests, concentrations of metal ions in the H_2SO_4 test solutions were gauged by ICP-MS; the

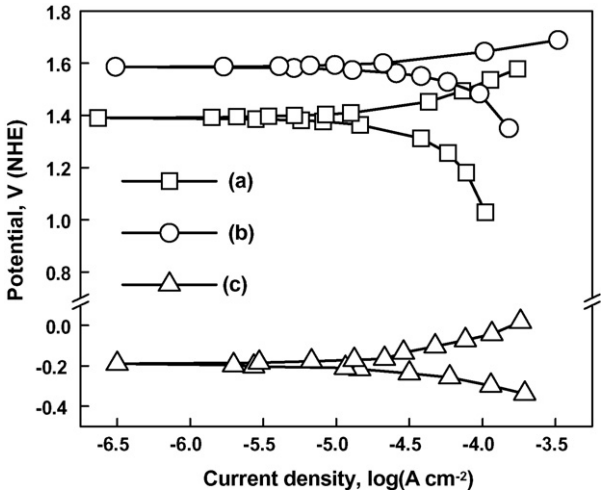

Fig. 7. Tafel curves of (a) Poco AXF-5QCF, (b) CFCSS developed under C_2H_2/H_2 ratio of 0.45 at 680 °C and (c) 304SS without carbon coating. Specimens were tested in 0.5 M H_2SO_4 solution at 25 °C.

results are consistent with the Tafel data obtained in Fig. 7. A considerable amount of metal ions (Fe: 8.175 ppm; Cr: 1.584 ppm; Ni: 1.725 ppm) were detected in the H_2SO_4 test solution of 304SS plate, suggesting that 304SS should corrode under PEMFC operating environment and liberate metal ions to contaminate the polymer electrolyte and Pt catalysts in PEMFC. Unlike 304SS plate, no metal ions were detected in the H_2SO_4 test solution of CFCSS plate, proving H_2SO_4 solution unable to penetrate through the carbon film to corrode 304SS substrate beneath. It is thus believed that the peak at 1.6 V is not related to the redox of CFCSS, but to the redox of H_2O on CFCSS surface, which is identical to the electrochemical reactions occurring on the surface of Poco graphite plate. The amazing result indeed demonstrates that the chemical stability of 304SS plate can be improved to the level of high-purity graphite plate by utilizing our CVD process to apply a carbon film on 304SS plate.

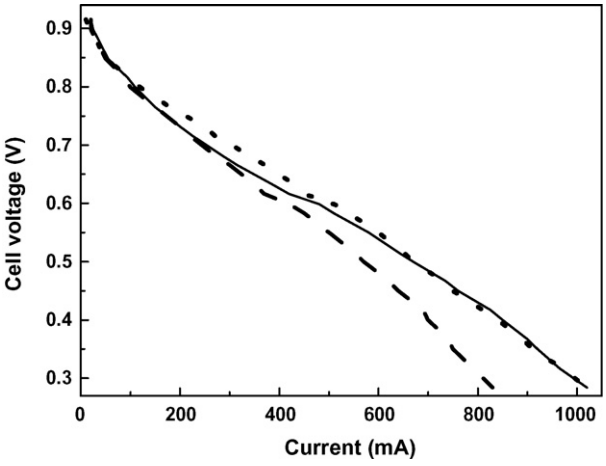

Fig. 8. Polarization curves of the fuel cells with (···) CFCSS bipolar plates, (—) Poco graphite bipolar plates and (- - -) 304SS bipolar plates after 100-h operation at 0.6 V and 40 °C.

Table 1
Surface resistance of the specimens gauged via four-point probe

Specimen	Sheet resistance ($\times 10^{-4}$ Ω/sq)
304SS plate	4.764
Poco graphite plate	6.224
CFCSS plate	4.805

3.4. Influence of bipolar plates on the performance of fuel cells

When PEMFC operation is performed at high temperature (above 60 °C), some problems, e.g. reactant gas humidifying, water flooding and product water-removing, arise and affect PEMFC performance seriously. To precisely evaluate the influence of anti-corrosivity of different bipolar plates on PEMFC performance, operating temperature of 40 °C was used to avoid the above effects and eliminate the variation of ambient temperature in the continuous 100-h PEMFC operation.

Fig. 8 shows the polarization curves of the fuel cell modules with different bipolar plates after 100-h operation at 0.6 V and 40 °C. The fuel cell with CFCSS bipolar plates demonstrates superior performance compared to that with 304SS bipolar plates. Although each fuel cell exhibited the same performance in the beginning, the current output of the fuel cell with 304SS bipolar plates gradually fell from 500 to 420 mA within 100 h, i.e. 16% loss in performance. According to the results observed in the corrosion endurance tests, it is supposed that 304SS bipolar plates liberate metal ions to contaminate Pt catalysts and proton-conductive membrane in the 100-h PEMFC operation. The declines in Pt catalytic activity and proton conductivity are responsible for the counteraction of 304SS bipolar plates to the PEMFC performance. The fuel cell with CFCSS bipolar plates manifested excellent stability in performance as that with Poco graphite bipolar plates during the 100-h operation. The similarity between their polarization curves in Fig. 8 provides the convincing evidence to verify the beneficial effect of the carbon film on protecting 304SS substrate against the corrosive environment in PEMFC.

It is surprising that the current output of the fuel cell with CFCSS bipolar plates is even higher than that with Poco graphite bipolar plates in the ohmic polarization region (0.5–0.8 V), as indicated in Fig. 8. This may be interpreted by the disparity between their electrical resistances (Table 1), as estimated via four-point probe measurement. Though the surface layer of the carbon film contains numerous disarranged graphite structures, the surface resistance of CFCSS plate is still lower than that of Poco graphite plate, suggesting that CFCSS bipolar plate can improve ohmic impedance in PEMFC operation. As expected, 304SS plate shows the lowest surface resistance in Table 1, but that hardly compensates for its poor chemical stability.

4. Conclusions

We have successfully improved the chemical stability of 304SS plate to the level of commercial graphite plate (Poco

AXF-5QCF) while maintaining its excellent electrical conductivity by CVD process to deposit a carbon film on Ni-coated 304SS plate. Surface morphology of the CVD deposited carbon strongly depends on the concentration of carbonaceous gas and a continuous carbon film with compact structure can be obtained at 680 °C under C_2H_2/H_2 mixed gas ratio of 0.45. Systematic analyses indicate that the carbon film displays a two layer structure, i.e. the highly ordered graphite layer at the carbon/Ni interface through the catalysis of Ni underlayer and the surface layer mainly containing disarranged graphite structures. The surface layer interrupts the migration paths of Ni atoms toward the surface of the carbon film, which results in the appearance of Ni precipitates inside the carbon film and further prevents the growth of filamentous carbon.

CFCSS plate delivers a much higher redox peak than 304SS plate in the corrosion endurance tests (1.6 versus −0.2 V), suggesting that CFCSS plates remain passive as graphite plate, but 304SS plates corrode under PEMFC operating environment. ICP-MS data for the H_2SO_4 test solution further prove that the carbon film completely isolates 304SS substrate from the corrosive environment while plenty of metal ions are liberated from the corrosion of 304SS plate. Working temperature of 40 °C is used in the continuous 100-h PEMFC operation to avoid the problems which usually occur at above 60 °C and seriously affect PEMFC performance, e.g. reactant gas humidifying, water flooding and product water-removing. As consistent with the results observed in the corrosion tests, the fuel cell with CFCSS bipolar plates demonstrated excellent stability in performance as compared to that with 304SS bipolar plates, which decayed 16% in performance after the 100-h running test at 0.6 V and 40 °C. The fuel cell with CFCSS bipolar plates performs slightly better than that with Poco graphite bipolar plates in the ohmic polarization region (0.5–0.8 V), responding to the lower surface resistance of the carbon film.

Overall, CFCSS bipolar plate displays excellent chemical stability in low temperature-operating PEMFC. To confirm the performance of CFCSS bipolar plate in high temperature-operating PEMFC, further tests with the help of ideal gas flow pattern, which efficiently improves water management at high temperature, are necessary.

References

[1] S. Gottesfeld, T.A. Zawodzinski, Adv. Electrochem. Sci. Eng. 5 (1997) 195.
[2] I. Bar-On, R. Kirchain, R. Roth, J. Power Sources 109 (2002) 71.
[3] J. Milliken, et al., Program overview Department of Energy Transportation Fuel Cell Program, 2000.
[4] D.N. Busick, M.S. Wilson, Fuel Cell Bull. 2 (1999) 6.
[5] J. Scholta, B. Rohland, V. Trapp, U. Focken, J. Power Sources 84 (1999) 231.
[6] H. Maeda, A. Yoshimura, H. Fukumoto, T. Hayashi, Abst. Fuel Cell Semin. (2002) 58.
[7] A. Heinzel, H. Kraus, C. Kreuz, F. Mahlendorf, O. Niemzig, Abst. Fuel Cell Semin. (2002) 153.
[8] A.B. LaConti, A.E. Griffith, C.C. Cropley, J.A. Kosek, US Patent 6,083,641 (2000).
[9] J. Wind, R. Spah, W. Kaiser, G. Bohm, J. Power Sources 105 (2002) 256.
[10] X. Cheng, B. Yi, M. Han, J. Zhang, Y. Qiao, J. Yu, J. Power Sources 79 (1999) 75.
[11] A. Pozio, R.F. Silva, M. De Francesco, L. Giorgi, Electrochim. Acta 48 (2003) 1543.
[12] H. Wang, M. Ann Sweikart, J.A. Turner, J. Power Sources 115 (2003) 243.
[13] E.A. Cho, U.-S. Jeon, H.Y. Ha, S.-A. Hong, I.-H. Oh, J. Power Sources 125 (2004) 178.
[14] E.A. Cho, U.-S. Jeon, et al., J. Power Sources 142 (2005) 177.
[15] R.F. Silva, D. Franch, et al., Electrochim. Acta 51 (2006) 3592.
[16] S.-J. Lee, J.-J. Lai, C.-H. Huang, J. Power Sources 145 (2005) 362.
[17] Y. Sone, H. Kishida, M. Kobayashi, et al., J. Power Sources 86 (2000) 334.
[18] H. March, A.P. Warburton, J. Appl. Chem. 20 (1970) 133.
[19] ASTM G5-94, Standard Reference Test Method for Marking Potentiostatic and Potentiodynamic Anodic Polarization Measurements.
[20] ASTM A262-79, Standard Recommended Practices for Detecting Susceptibility to Intergranular Attack in Stainless Steels, 2000.
[21] J.C. Shelton, J.R. Patil, J.M. Blakeley, Surf. Sci. 43 (1974) 493.
[22] A.I. Boronin, V.I. Bukhtiyarov, R. Kvon, V.V. Chesnokov, R.A. Buyanov, Surf. Sci. 258 (1991) 289.
[23] C.M. Chun, J.D. Mumford, T.A. Ramanarayanan, J. Electrochem. Soc. 147 (2000) 3680.
[24] W.N. Turnar, F.C. Jolinson, J. Appl. Polym. Sci. 13 (1969) 2073.
[25] J. Kastner, T. Pichler, H. Kuzmany, S. Curran, W. Blau, D.N. Weldon, M. Delamesiere, S. Draper, H. Zandbergen, Chem. Phys. Lett. 221 (1994) 53.